OSSERVATORIO ASTROFISICO DI CATANIA

Reliability Test of all 37 SiPM I/F Boards of the ASTRI SST-2M Camera through Pulse Height Distribution Measurements

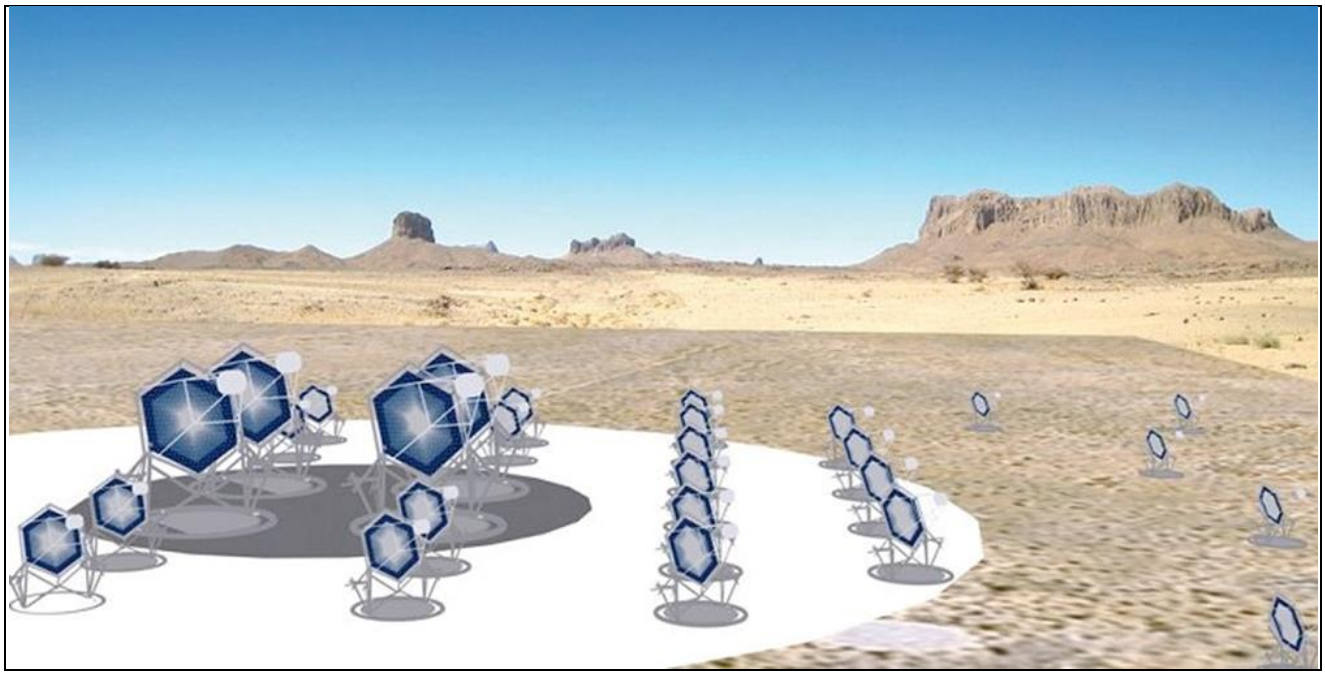

Osservatorio Astrofisico di Catania

G. ROMEO[(1)], S. GAROZZO[(1)], D. MARANO[(1)], G. BONANNO[(1)], A. GRILLO[(1)], M. C. TIMPANARO[(1)]

(1) INAF – Osservatorio Astrofisico di Catania

Rapporti interni e tecnici
N. 6/2014

INAF - Osservatorio Astrofisico di Catania
Via Santa Sofia, 78 I-95123 Catania, Italy Tel.: +39- 095-7332 111 Fax: +39-095-330592
Sede "Mario G.Fracastoro" (Etna) – Tel +39-095-911580 Fax+39-095-916184
www.oact.inaf.it - oacatania@oact.inaf.it

Reliability Test of all 37 SiPM I/F Boards of the ASTRI SST-2M Camera through Pulse Height Distribution Measurements

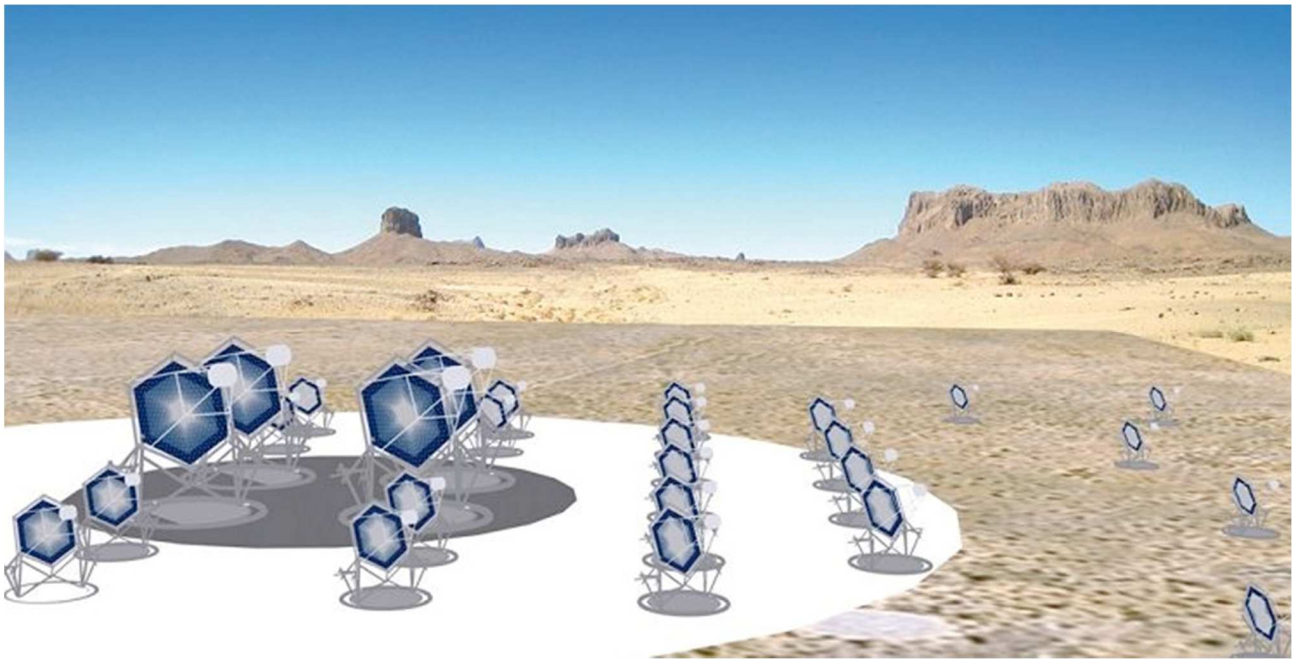

Prepared by: Name: Giuseppe Romeo, Salvatore Garozzo, Davide Marano Signature: Date: 25/07/2014

Reviewed by: Name: Giovanni Bonanno Signature Date: 25/07/2014

Approved by: Name: Giovanni Bonanno Signature: Date: 25/07/2014

TABLE OF CONTENTS

DISTRIBUTION LIST

ASTRI mailing list	astri@brera.inaf.it
Bruno Sacco	bruno.sacco@iasf-palermo.inaf.it
Giovanni Pareschi	giovanni.pareschi@brera.inaf.it
Stefano Vercellone	stefano@ifc.inaf.it
Rodolfo Canestrari	rodolfo.canestrari@brera.inaf.it
Osvaldo Catalano	osvaldo.catalano@iasf-palermo.inaf.it
Enrico Cascone	cascone@na.astro.it
Giovanni La Rosa	larosa@ifc.inaf.it
Giovanni Bonanno	gbo@oact.inaf.it
Giuseppe Romeo	giuseppe.romeo@oact.inaf.it
Sergio Billotta	sergio.billotta@oact.inaf.it
Patrizia Caraveo	pat@lambrate.inaf.it
Davide Marano	davide.marano@oact.inaf.it
Alessandro Grillo	agrillo@oact.inaf.it
Luca Stringhetti	luca@iasf-milano.inaf.it
Rachele Millul	rachele.millul@brera.inaf.it
Mauro Fiorini	fiorini@lambrate.inaf.it
Salvatore Garozzo	salvatore.garozzo@oact.inaf.it
Domenico Impiombato	domenico.impiombato@ifc.inaf.it
Giuseppe Sottile	sottile@ifc.inaf.it
Salvatore Giarrusso	jerry@ifc.inaf.it
ASTRI mailing list	astri@brera.inaf.it

DOCUMENT HISTORY

Version	Date	Modification
1.0	Date	first version
		update

LIST OF ACRONYMS

OACT	Osservatorio Astrofisico di Catania
IFC	Istituto di Astrofisica Spaziale e Fisica Cosmica di Palermo
COLD	Catania astrophysical Observatory Laboratory for Detectors
PCB	Printed Circuit Board
SiPM	Silicon Photo-Multiplier
MPPC	Multi Pixel Photon Counter
SST-2M	Small-Size Telescope Dual-Mirror
PDM	Photon Detection Module
ASIC	Application Specific Integrated Circuit
FEE	Front-End Electronics
BEE	Back-End Electronics
FPGA	Field Programmable Gate Array
EASIROC	Extended Analogue Silicon-pm Integrated Read-Out Chip
CITIROC	Cherenkov Imaging Telescope Integrated Read-Out Chip
I/F	Interface

APPLICABLE DOCUMENTS

[AD1]

REFERENCE DOCUMENTS

[R1] Distribuzione delle PDM sul piano focale della camera ASTRI e layout di ogni singola PDM – code: ASTRI-TR-OACT-3200-012.

[R2] Systematic Calibration Procedure for the Temperature Sensors of the SiPM Interface Board – code: ASTRI-TR-OACT-3200-013.

[R3] SiPM Interface Systems for the Characterization of Complete PDMs of the ASTRI SST-2M Camera – code: ASTRI-TR-OACT-3200-014.

1. INTRODUCTION

This document is intended to report on the reliability tests, performed at the COLD laboratory, for the SiPM macro-pixels of an entire photon detection module (PDM) at the focal plane of the ASTRI SST-2M telescope through the pulse height distribution method. Measurements carried out are aimed at testing the SiPM boards in terms of assembling and production.

Pulse height distributions are not the final target, but represent an effective tool to evaluate the functionality of the SiPM macro-pixels and check the board design and the detector soldering technique.

In particular, the complete measurements system is first addressed; subsequently, the focal plane arrangement is described, and the charge distribution plots are reported.

In addition, the pulse height distribution for a new $3\times3mm^2$ Hamamatsu detector is provided in this report to provide measurement comparison.

All measurements are performed in dark conditions.

2. MEASUREMENT SYSTEM

The instrumental apparatus developed at the COLD laboratory has been envisaged to provide a systematic characterization of each SiPM board constituting the camera focal plane of the ASTRI SST-2M telescope prototype.

Charge distributions measurements for the ASTRI focal plane PDMs are obtained by means of two testing systems:

1. the electronic board developed at the COLD laboratory, called “adapter board”, used for SiPM macro-pixels preliminary tests;
2. the EASIROC evaluation board, provided by OMEGA, for SiPM read-out.

EASIROC (Extended Analogue Silicon-photomultiplier Read-Out Chip) is a 32-channel fully analogue front end ASIC produced by OMEGA and dedicated to the gain trimming and read-out of the ASTRI MPPC detectors signals. The EASIROC chip is soldered onto a dedicated evaluation board providing 32 external inputs for the MPPC signals. The EASIROC evaluation board is depicted in Fig. 1.

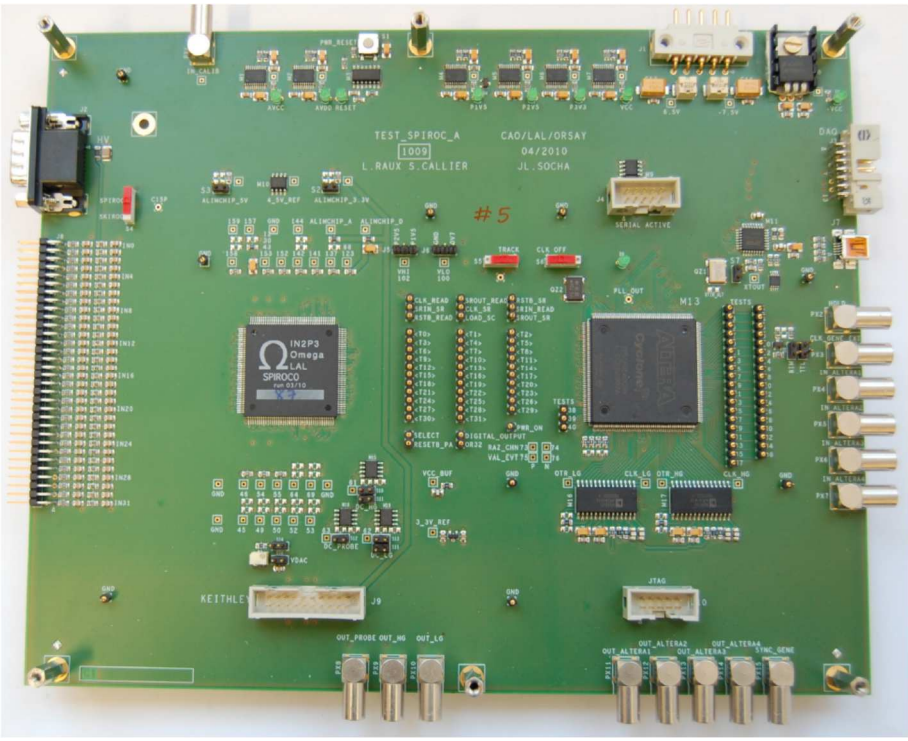

Fig. 1. EASIROC evaluation board (realized by Omega).

To allow a versatile interface between the silicon photomultiplier signals of the logical PDM pixels and the EASIROC evaluation board, an adapter board has been realized at

the COLD laboratory, to interface the PCB hosting the PDM camera detectors with the EASIROC evaluation board. The PCB of the realized adapter board are illustrated in Fig. 2 and in Fig. 3, respectively for the top and bottom side.

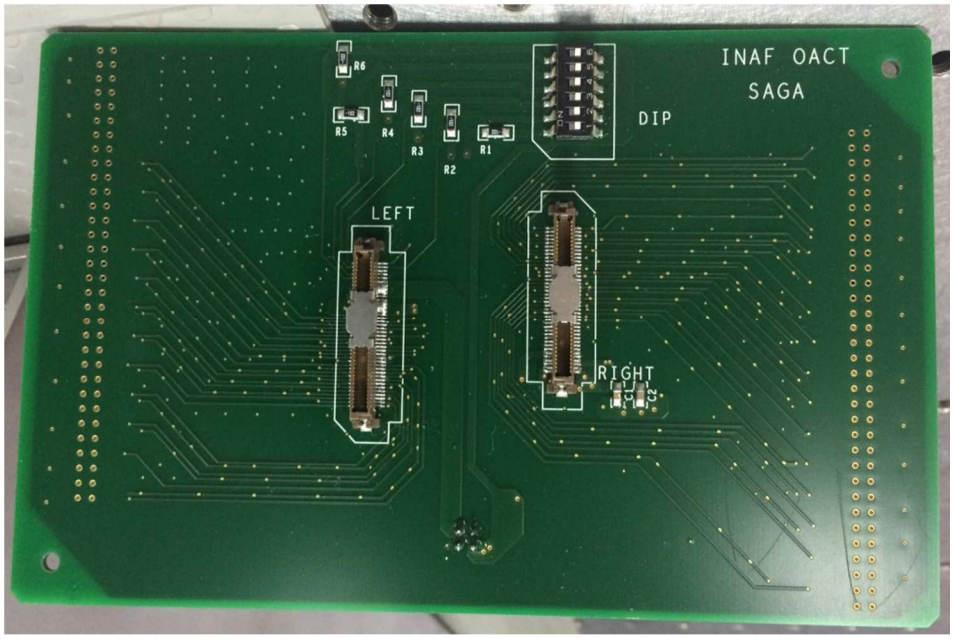

Fig. 2. Top layer printed circuit of the realized adapter board.

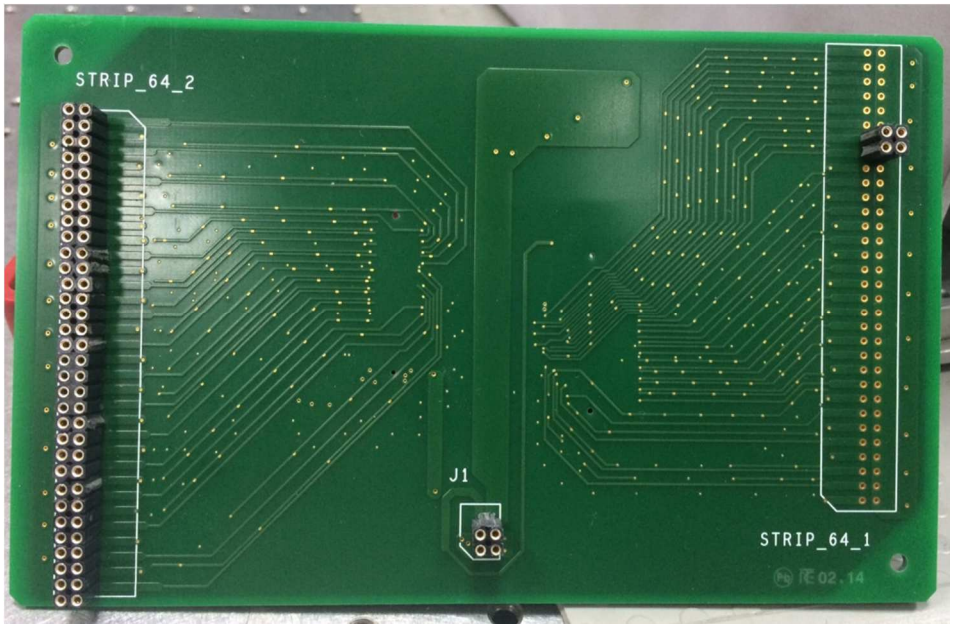

Fig. 3. Bottom layer printed circuit of the realized adapter board.

A specific mechanical support is realized to house the MPPC board; in particular, the black light-tight prevents accidental light exposure of the MPPC detectors and allows a thermal stabilization. The temperature control of the SiPM I/F is obtained through a cooling system designed at the COLD laboratory of INAF-OACT, based on a Peltier cell whose hot side is cooled by a CPU fan (see Fig. 4).

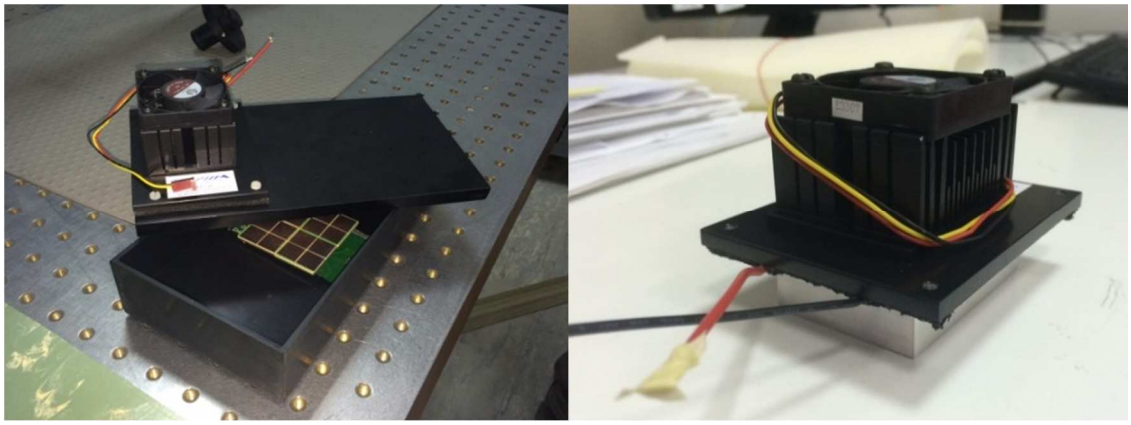

Fig. 4. The left side shows the box hosting the adapter board and the SiPM I/F board connected onto it. On the right side, the thermoelectric cooler based on a Peliter cell is depicted.

The complete experimental apparatus that has been exploited for pulse height distribution measurements is illustrated in Fig. 5, also showing the measurement instruments involved.

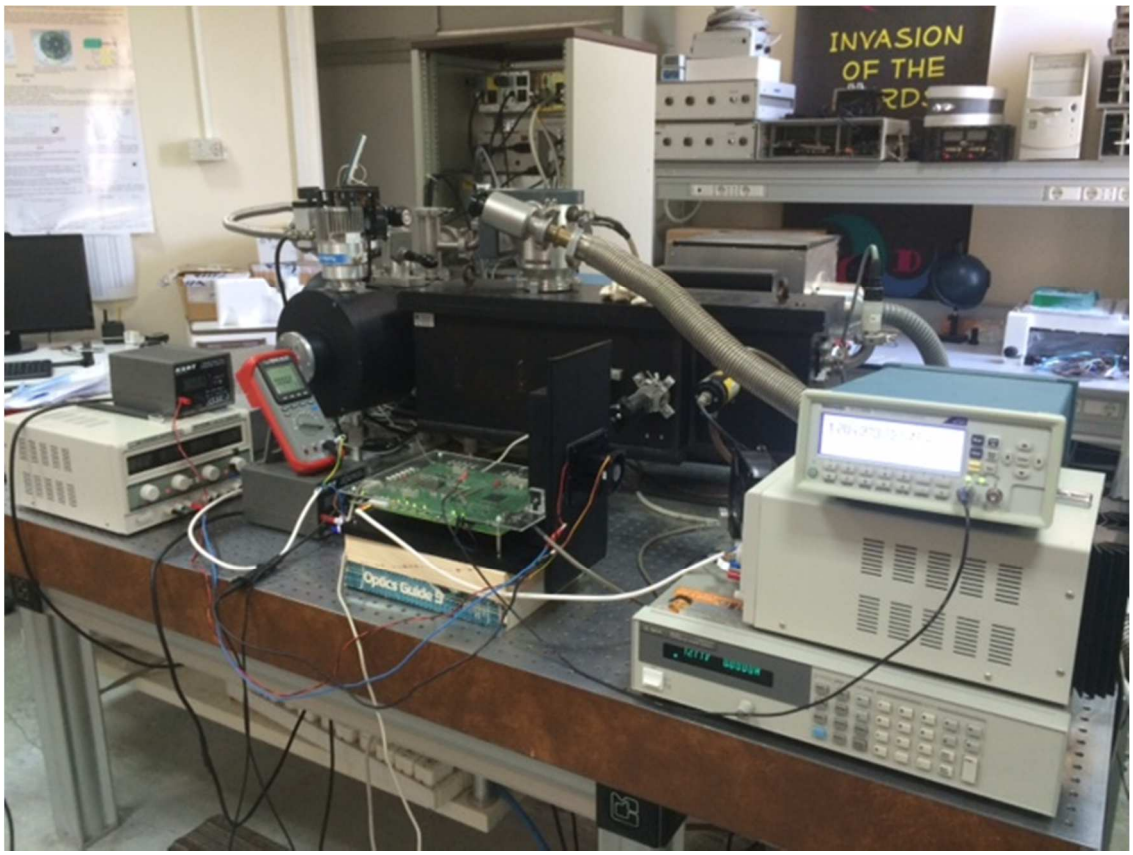

Fig. 5. Complete instrumental apparatus exploited for pulse height distribution measurements.

3. FOCAL PLANE STRUCTURE

In the following, the pulse height distribution results of the SiPM macro-pixel of the focal plane are reported. The various SiPM boards numbers are referenced through the distribution schematization depicted in Fig. 6 [R1].

The reference position of SiPMs and logical macro-pixels for each single PDM unit is illustrated in Fig. 7.

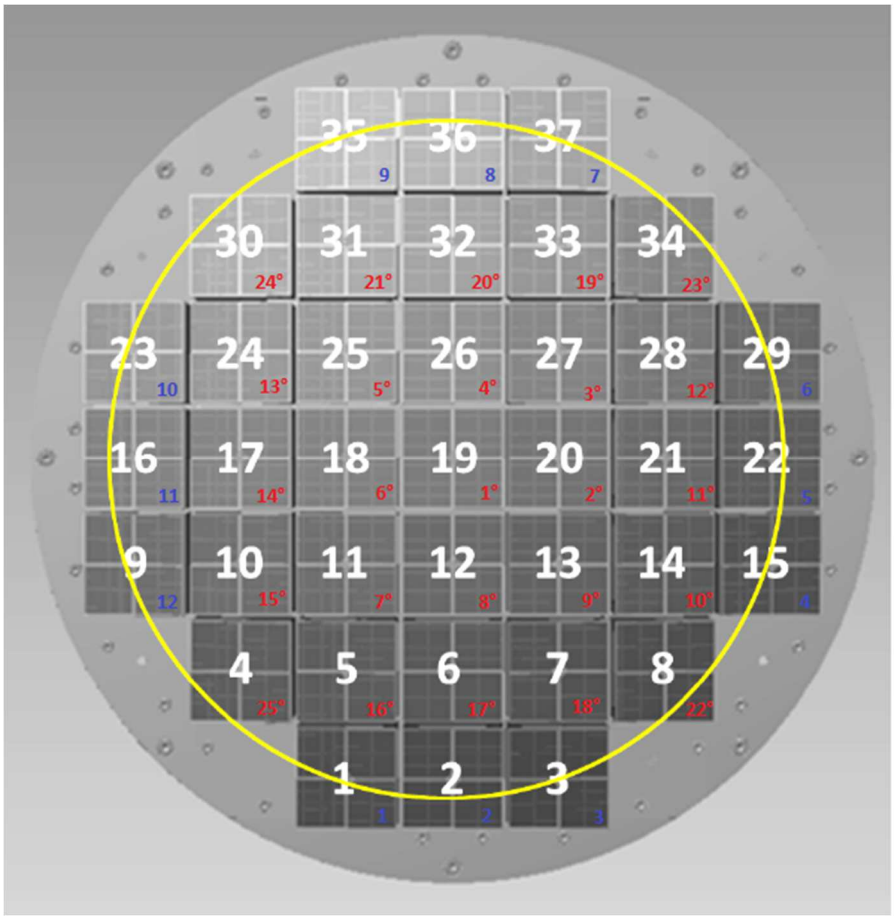

Fig. 6. PDM reference distribution at the focal plane of the ASTRI SST-2M camera.

The SiPM interface board with the assembled MPPC detectors on the top layer is depicted in Fig. 8.

Composing each of the 37 SiPM boards side by side yields the ASTRI focal plane structure illustrated in Fig. 9. An alternative and more realistic representation of the focal plane is provided in Fig. 10, with simulated inter-spaces among each SiPM board.

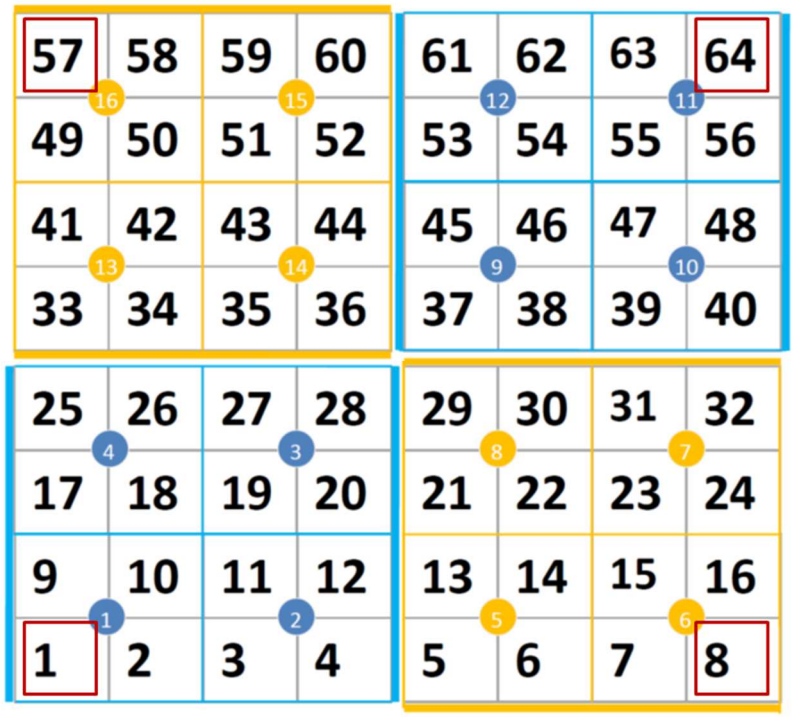

Fig. 7. SiPMs and macro-pixel reference position for each single PDM unit.

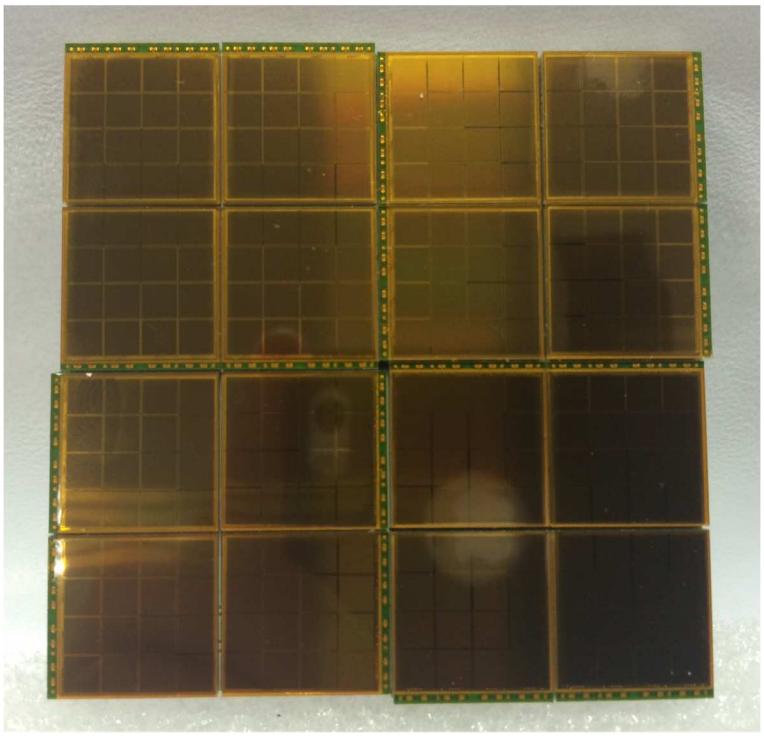

Fig. 8. SiPM interface board with the assembled MPPC detectors on the top layer.

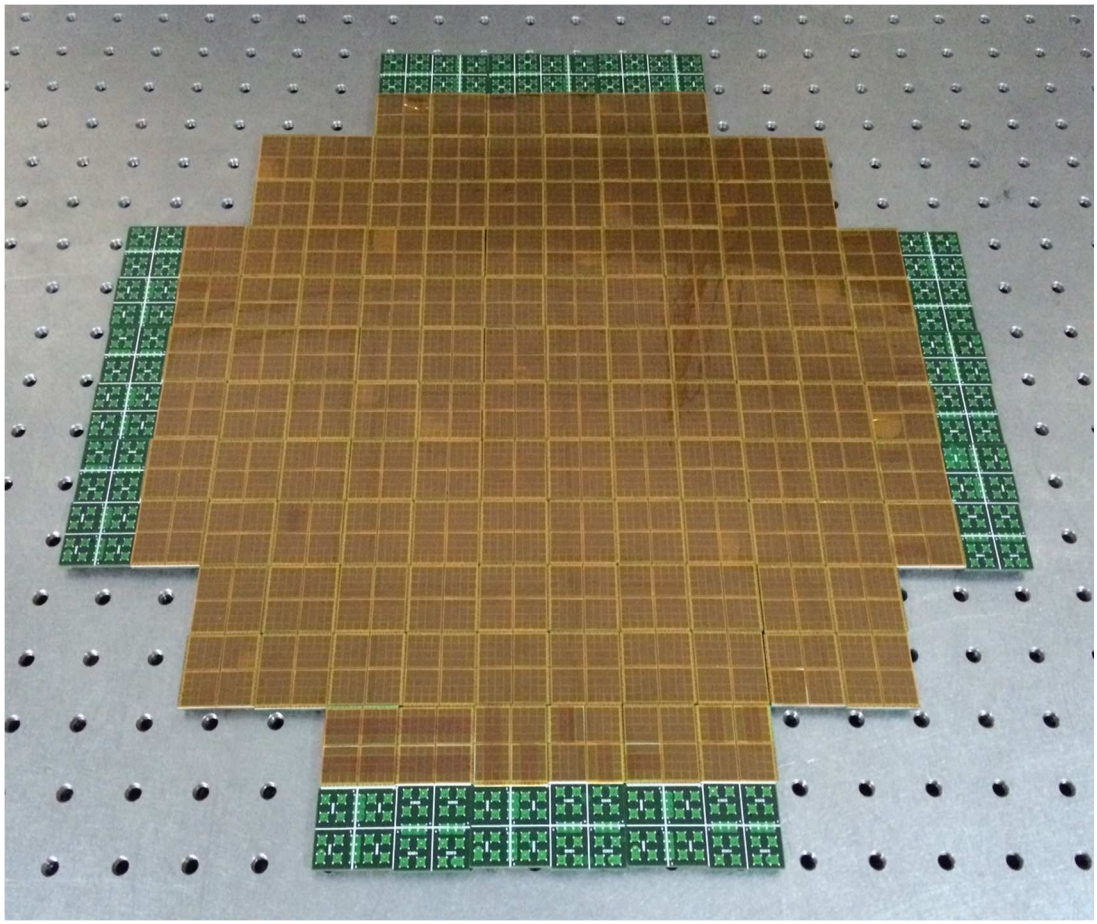

Fig. 9. ASTRI focal plane composition, showing the 37 PDM units.

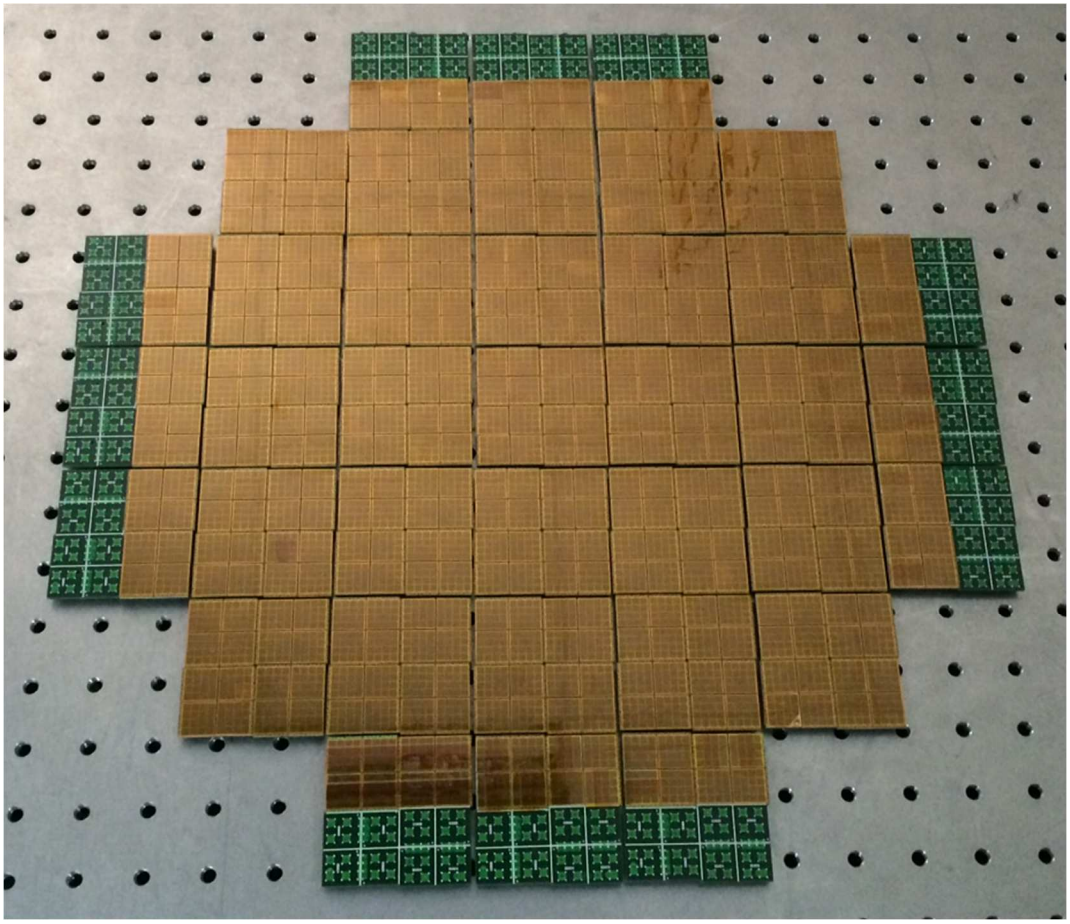

Fig. 10. ASTRI focal plane with inter-spaces among each SiPM interface board.

4. PDM MACRO-PIXEL PULSE HEIGHT DISTRIBUTIONS

In the following, pulse height distribution results of various sample SiPM macro-pixels from different PDMs are reported. For each measurement, the operating voltage V_{OP} biasing the SiPMs is finely tuned with respect to the nominal value, in order to achieve optimal sensor gain. In addition, the DAC value regulating the discriminator threshold is opportunely chosen in order to avoid as much as possible the superimposition of the electronic noise, whose influence has been evaluated for the corresponding channels.

PDMs and SiPM macro-pixels referenced throughout these distributions are numbered as they are represented in Fig. 6 and Fig. 7.

Low temperature values (from 8°C to 10°C) and nominal operating voltages have been kept to reduce as much as possible the dark noise of the SiPM macro-pixels and achieve higher overvoltage values (and in turn higher gain).

Indeed, due to the low gain value of the MPPC detectors (7.5×10^5) and the EASIROC fast shaper gain stage (unable to provide sufficient amplification, being designed to drive detectors with gains in the order of 10^6), and because of the grouping of four 3mm×3mm SiPM pixels, the resulting pulse amplitude turns out to be poor to achieve good photoelectron resolution in the pulse height distribution plots.

PDM 04

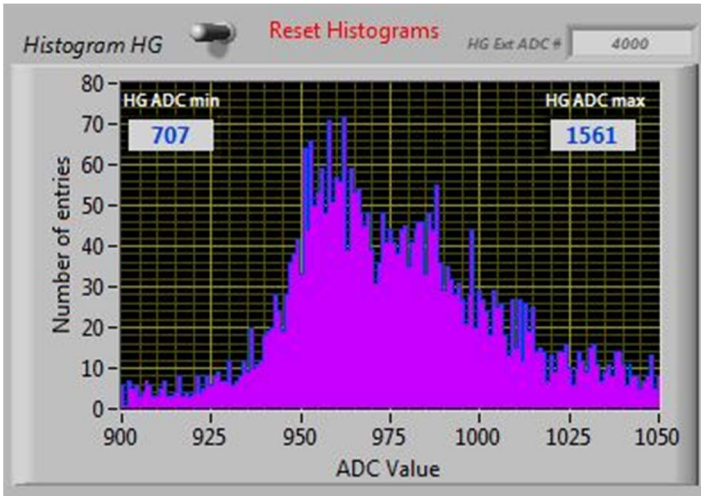

Fig. 11. Pulse height distribution of the macro-pixel 27 at T=8.4°C (V_{OP}=73.03V, DAC=852ch).

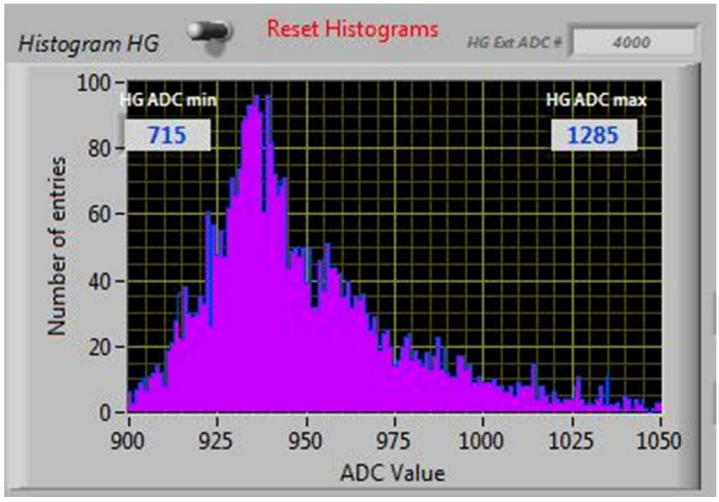

Fig. 12. Pulse height distribution of the macro-pixel 28 at T=8.4°C (V_{OP}=72.34V, DAC=858ch).

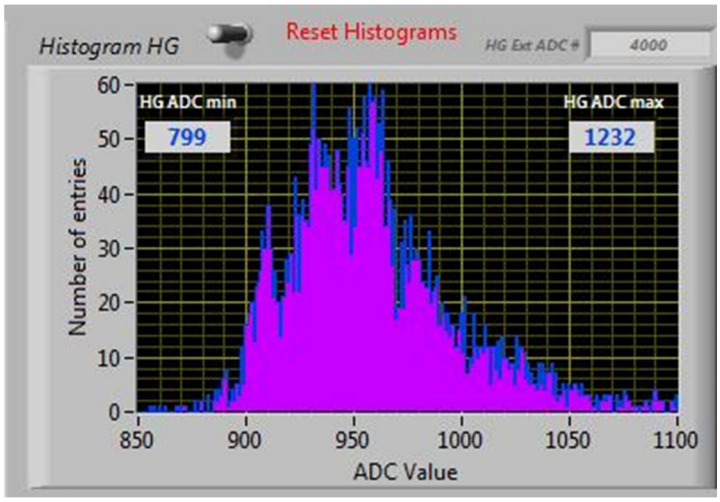

Fig. 13. Pulse height distribution of the macro-pixel 29 at T=8.4°C (V_{OP}=72.30V, DAC=845ch).

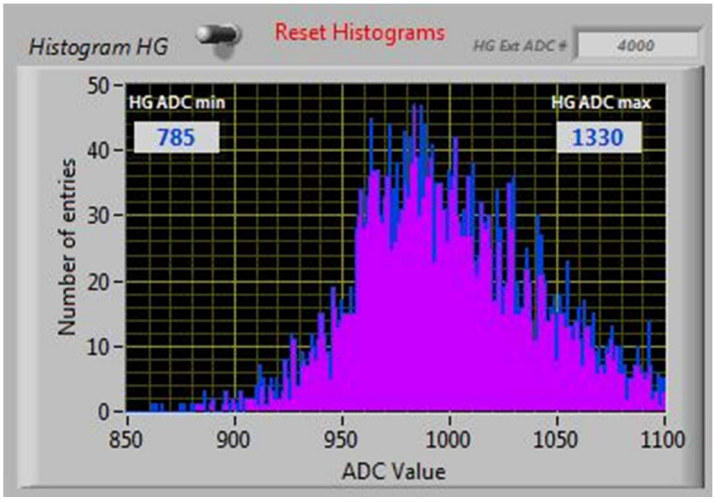

Fig. 14. Pulse height distribution of the macro-pixel 30 at T=8.4°C (V_{OP}=72.50V, DAC=826ch).

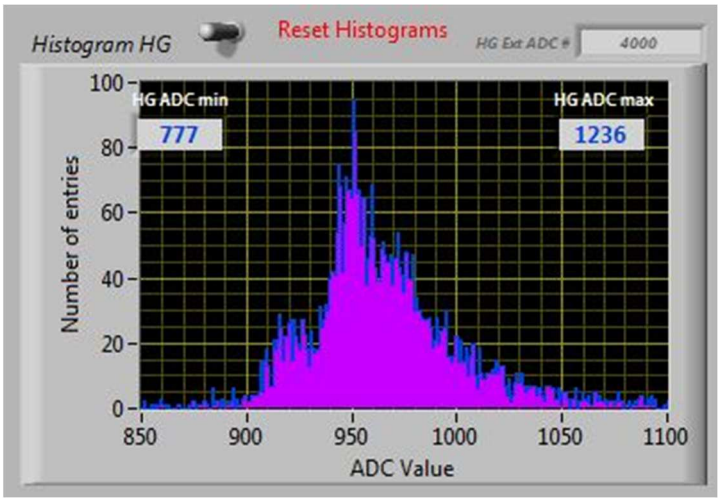

Fig. 15. Pulse height distribution of the macro-pixel 36 at T=8.4°C (V_{OP}=72.85V, DAC=853ch).

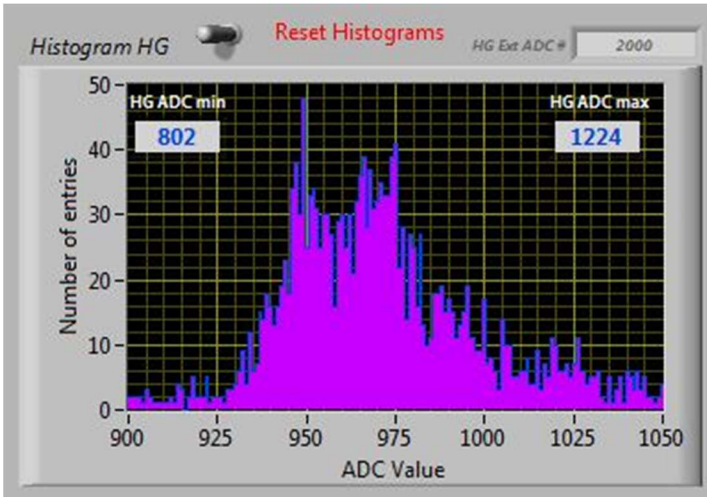

Fig. 16. Pulse height distribution of the macro-pixel 30 at T=9.3°C (V_{OP}=72.75V, DAC=852ch).

PDM 30

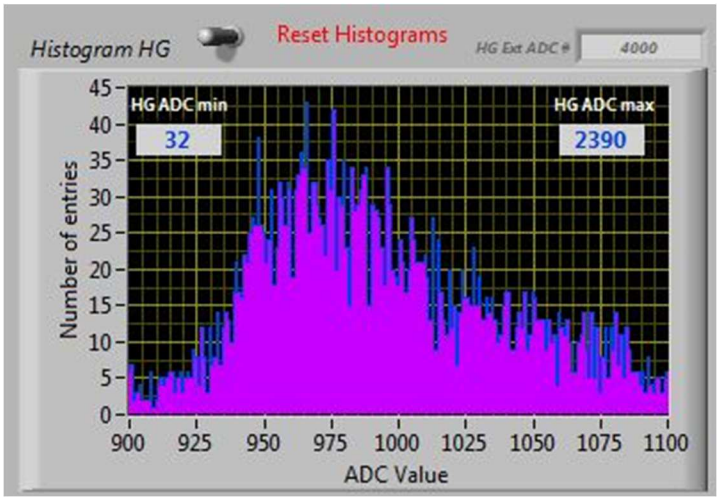

Fig. 17. Pulse height distribution of the macro-pixel 28 at T=9.3°C (V_{OP}=72.32V, DAC=853ch).

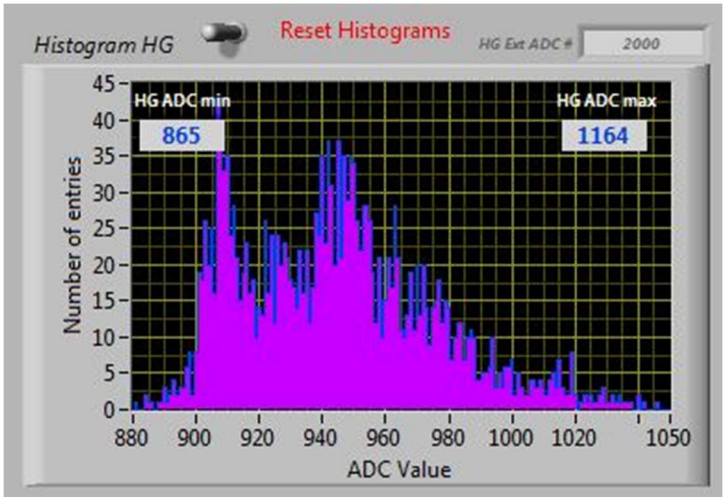

Fig. 18. Pulse height distribution of the macro-pixel 29 at T=10°C (V_{OP}=72.00V, DAC=845ch).

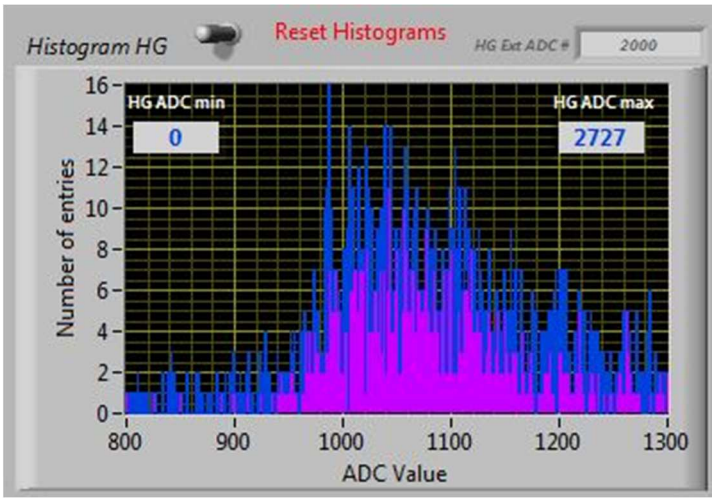

Fig. 19. Pulse height distribution of the macro-pixel 36 at T=10°C (V_{OP}=72.50V, DAC=832ch).

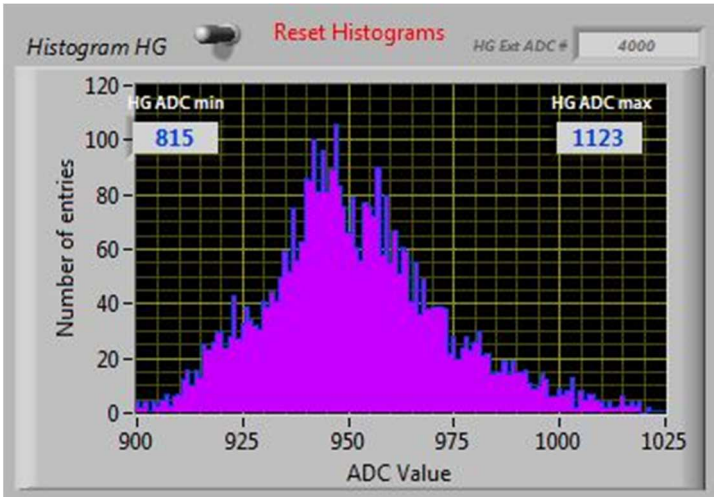

Fig. 20. Pulse height distribution of the macro-pixel 37 at T=10°C (V_{OP}=71.60V, DAC=858ch).

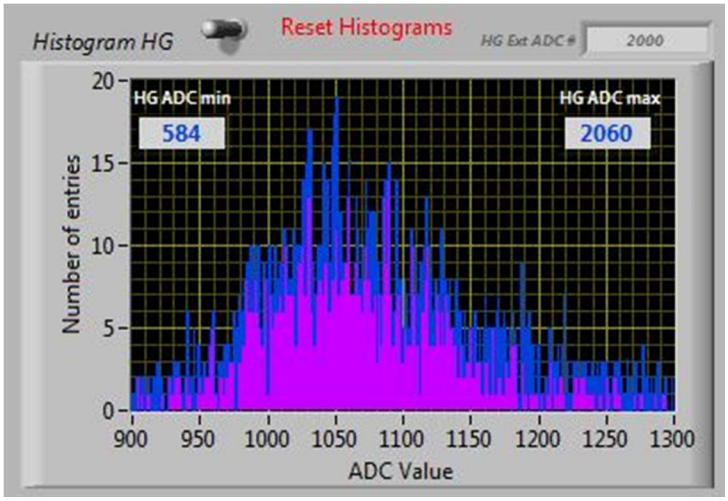

Fig. 21. Pulse height distribution of the macro-pixel 44 at T=9.5°C (V_{OP}=72.22V, DAC=805ch).

PDM 34

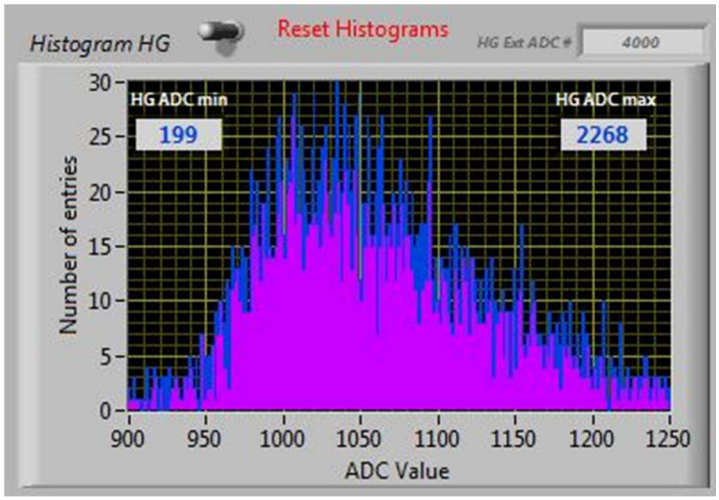

Fig. 22. Pulse height distribution of the macro-pixel 29 at T=9°C (V_{OP}=73.00V, DAC=819ch).

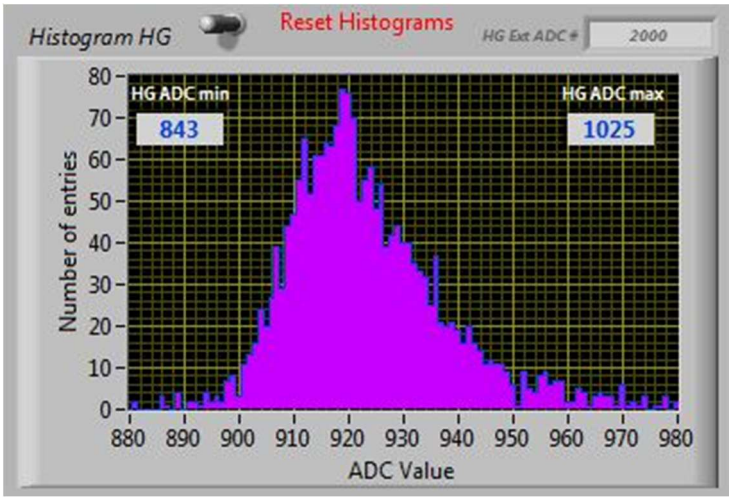

Fig. 23. Pulse height distribution of the macro-pixel 36 at T=9°C (V_{OP}=72.32V, DAC=832ch).

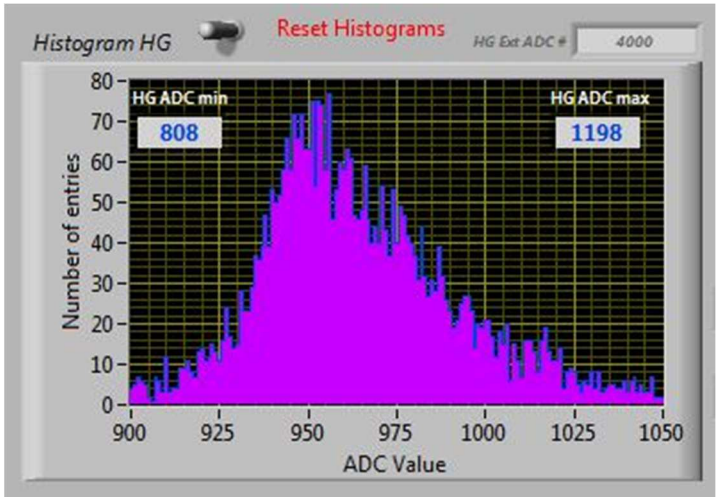

Fig. 24. Pulse height distribution of the macro-pixel 37 at T=9°C (V_{OP}=72.90V, DAC=854ch).

PDM 12

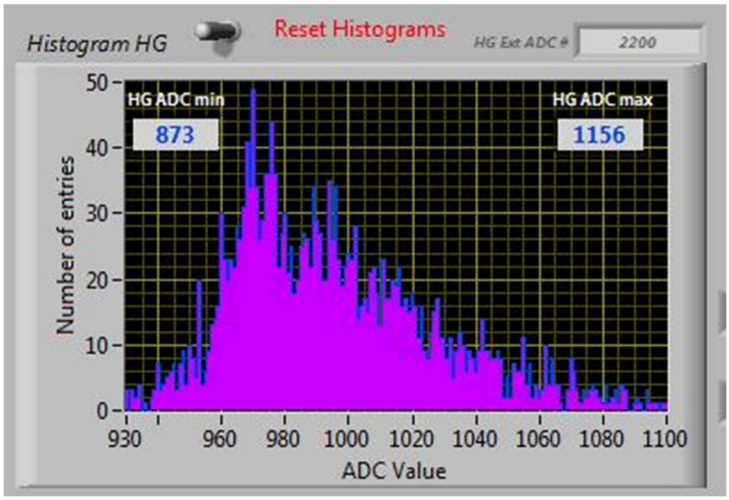

Fig. 25. Pulse height distribution of the macro-pixel 30 at T=10°C (V_{OP}=72.00V, DAC=824ch).

PDM 19

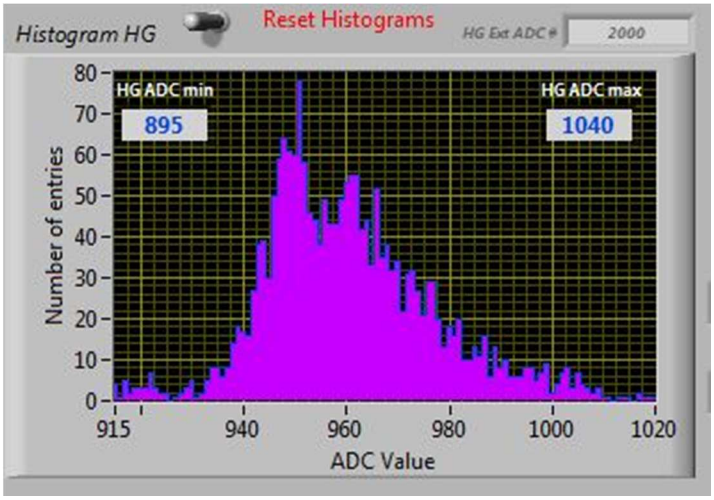

Fig. 26. Pulse height distribution of the macro-pixel 60 at T=10°C (V_{OP}=72.40V, DAC=832ch).

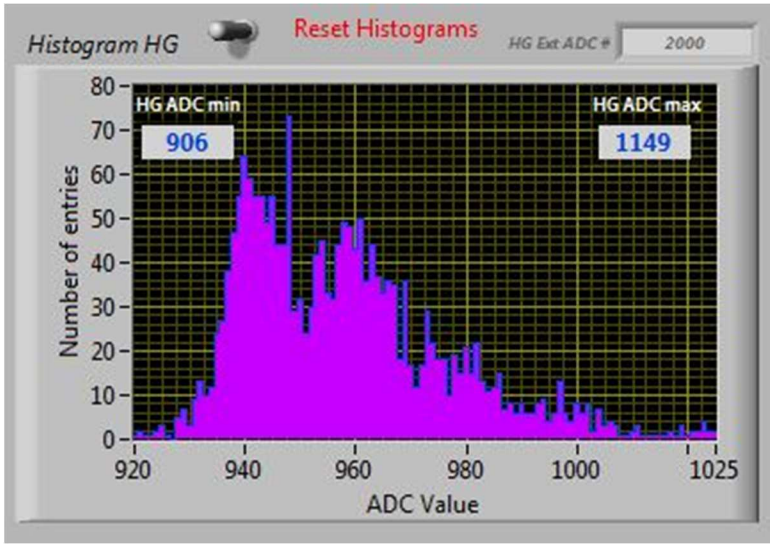

Fig. 27. Pulse height distribution of the macro-pixel 20 at T=10°C (V_{OP}=72.40V, DAC=854ch).

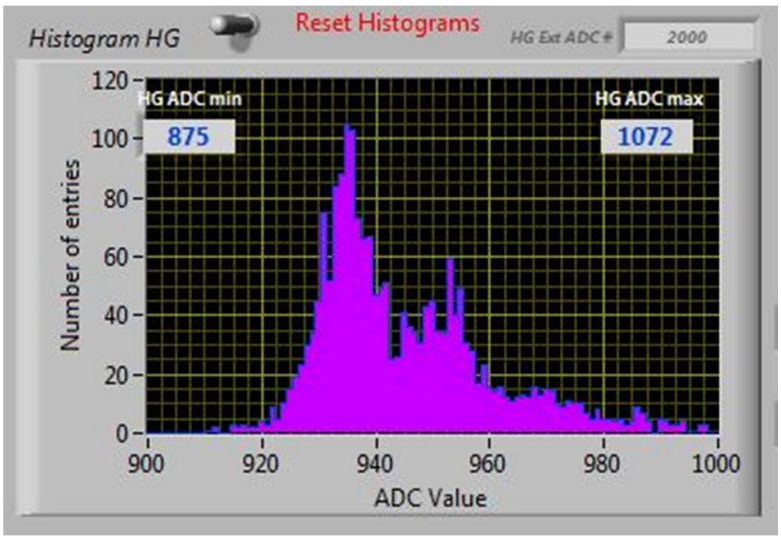

Fig. 28. Pulse height distribution of the macro-pixel 35 at T=10°C (V_{OP}=72.90V, DAC=857ch).

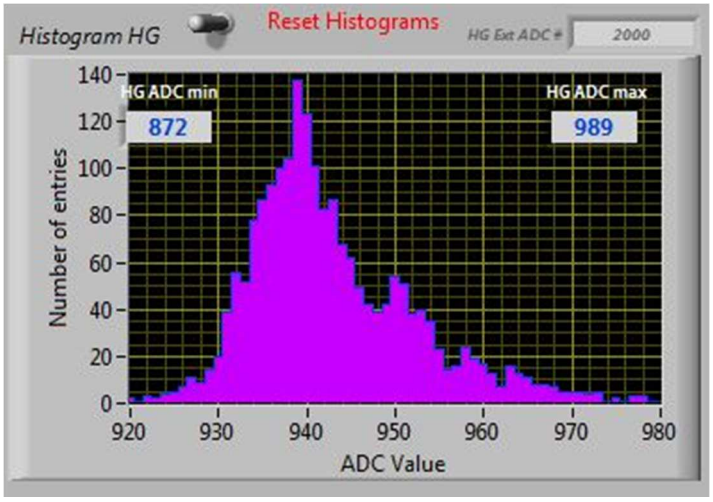

Fig. 29. Pulse height distribution of the macro-pixel 01 at T=10°C (V_{OP}=72.40V, DAC=861ch).

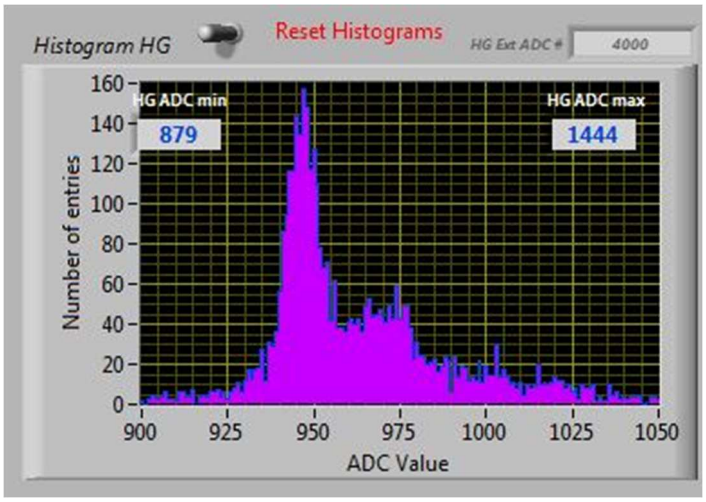

Fig. 30. Pulse height distribution of the macro-pixel 37 at T=10°C (V_{OP}=72.80V, DAC=856ch).

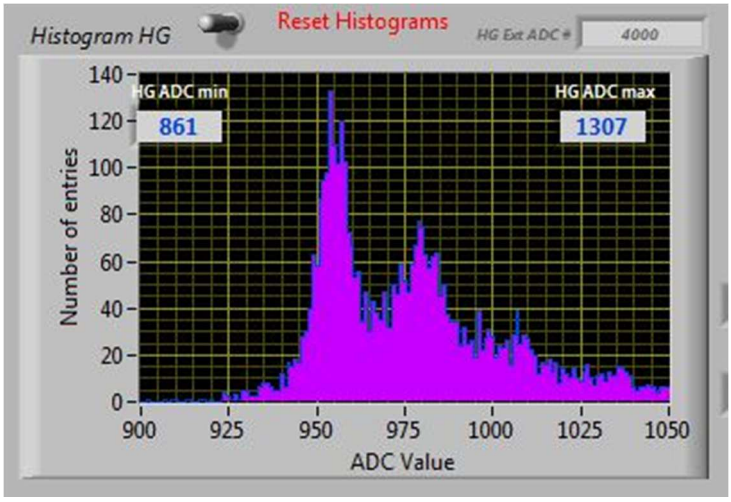

Fig. 31. Pulse height distribution of the macro-pixel 38 at T=10°C (V_{OP}=72.80V, DAC=853ch).

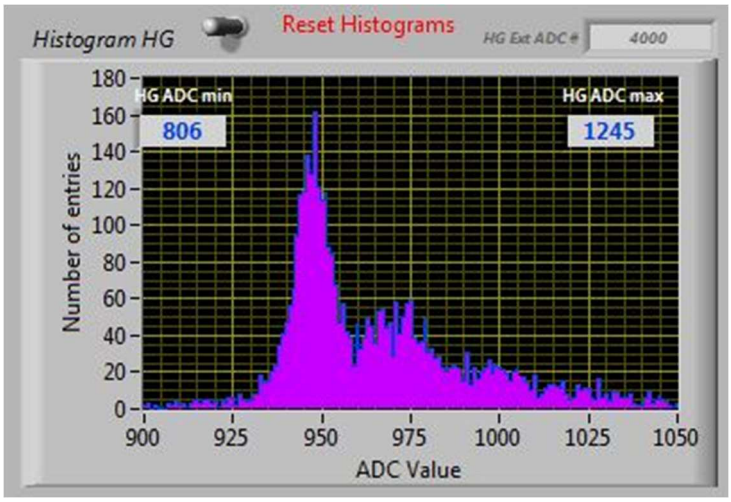

Fig. 32. Pulse height distribution of the macro-pixel 45 at T=10°C (V_{OP}=72.80V, DAC=853ch).

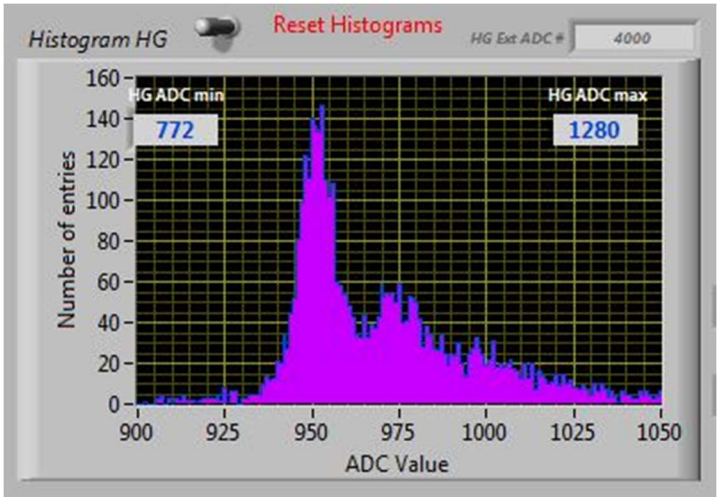

Fig. 33. Pulse height distribution of the macro-pixel 46 at T=10°C (V_{OP}=72.80V, DAC=891ch).

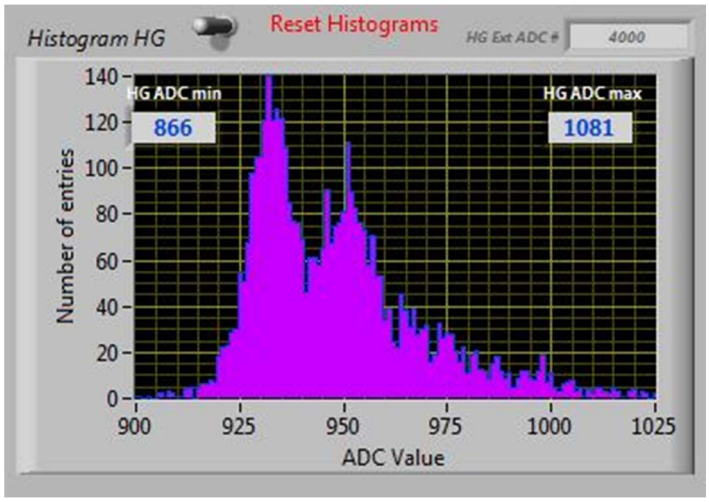

Fig. 34. Pulse height distribution of the macro-pixel 08 at T=10°C (V_{OP}=72.00V, DAC=857ch).

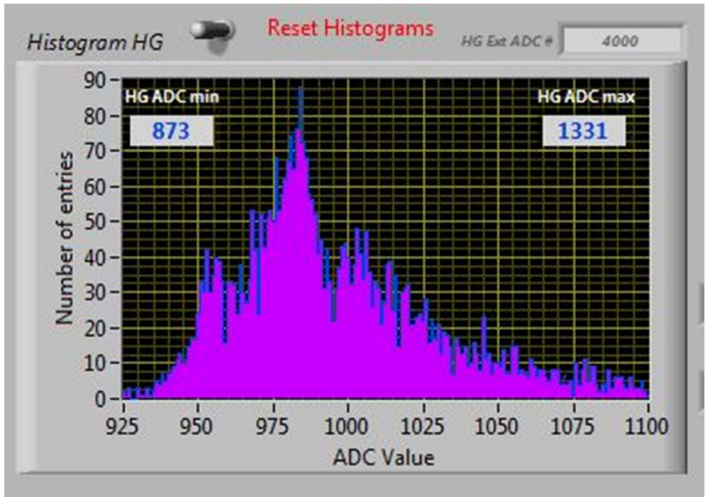

Fig. 35. Pulse height distribution of the macro-pixel 64 at T=10°C (V_{OP}=72.60V, DAC=847ch).

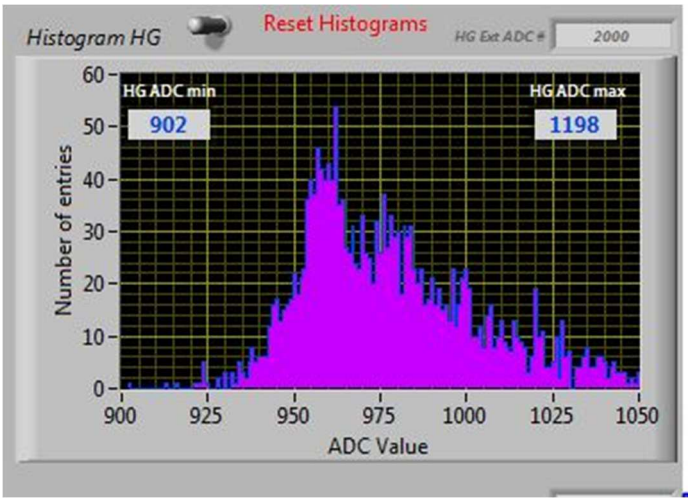

Fig. 36. Pulse height distribution of the macro-pixel 21 at T=10°C (V_{OP}=72.40V, DAC=844ch).

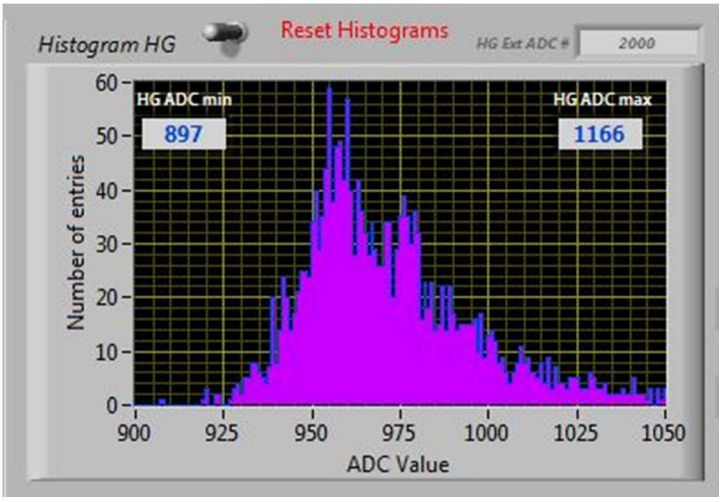

Fig. 37. Pulse height distribution of the macro-pixel 22 at T=10°C (V_{OP}=72.40V, DAC=848ch).

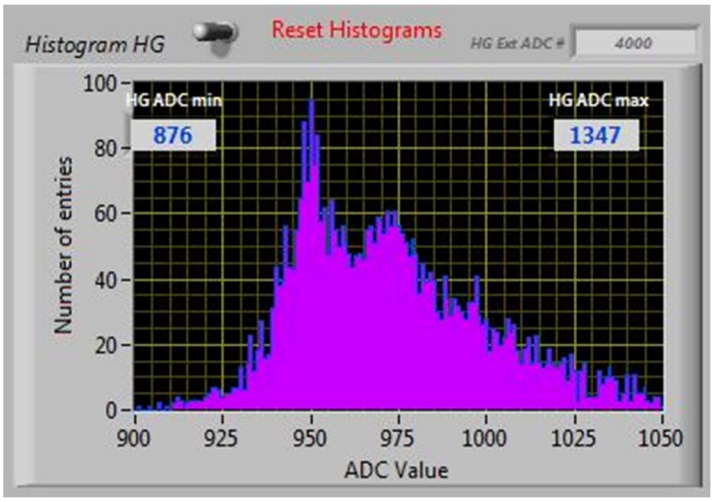

Fig. 38. Pulse height distribution of the macro-pixel 29 at T=10°C (V_{OP}=72.40V, DAC=844ch).

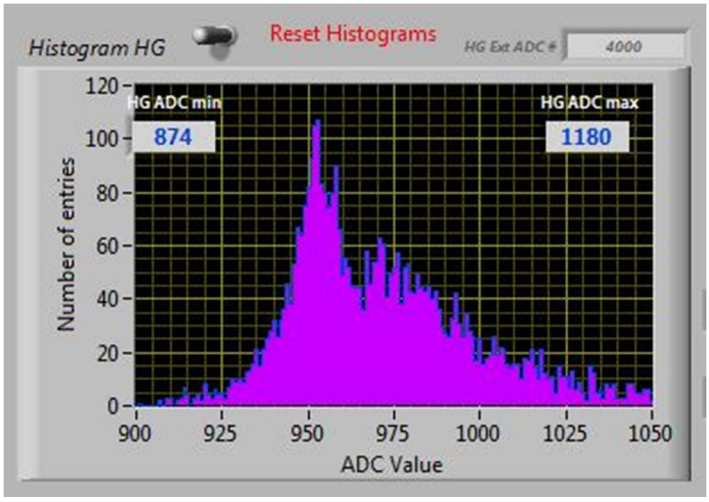

Fig. 39. Pulse height distribution of the macro-pixel 30 at T=10°C (V_{OP}=72.40V, DAC=838ch).

As it results from the above screenshots, photoelectron resolution of the pulse height distributions is not sufficiently good for all the tested PDMs, because of the above mentioned problems.

5. PULSE HEIGHT MEASUREMENTS WITH A DIFFERENT SIPM

Pulse height distributions are also carried out with the same electronics for a different SiPM detector, to confirm the quality of the SiPM boards and confirm the functionality of the testing procedure.

A 3×3mm^2 Hamamatsu LCT-1 detector with a higher gain (1.47×10^6) has been soldered in one of the 64 available channels in the PDM test board. In particular, its anode and cathode terminals have been connected to one channel of the EASIROC electronics by means of the COLD adapter board, as shown in Fig. 40 and Fig. 41.

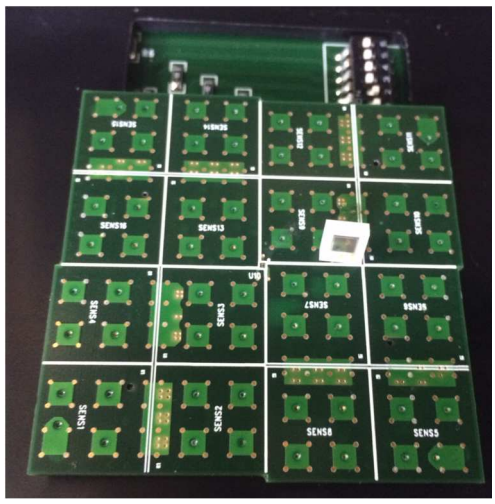

Fig. 40. Hamamatsu LCT-1 SiPM detector connected to the PDM test board.

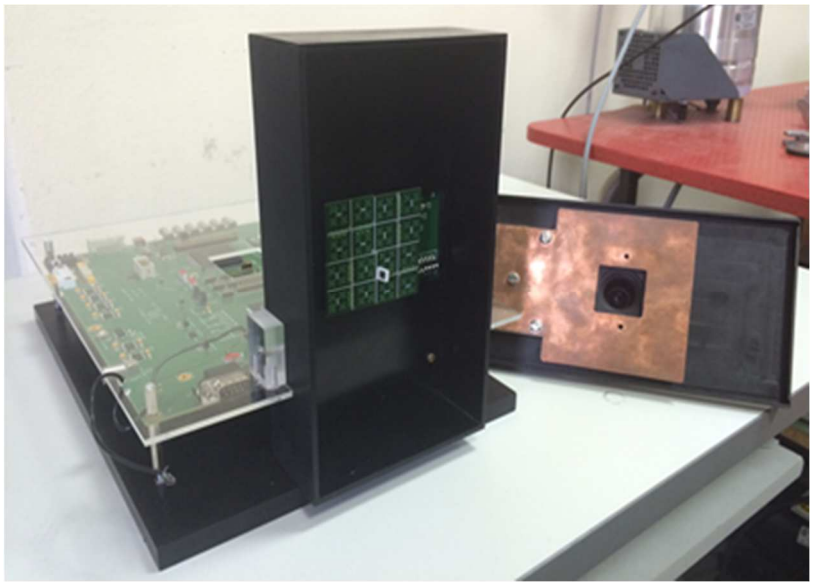

Fig. 41. Black box with the LCT-1 detector connected to the EASIROC evaluation board.

Pulse height distributions are also carried out for the analyzed LCT-1 detector at 25°C and for V_{OP}=57.46V. Measurement results are shown in Fig. 42.

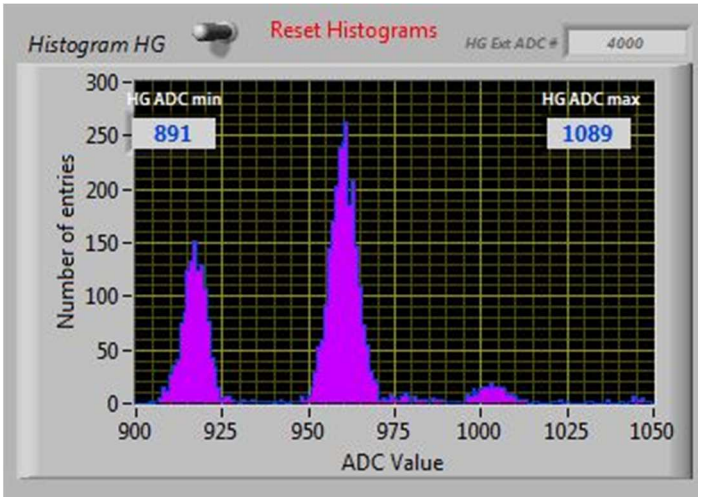

Fig. 42. Pulse height distribution of the macro-pixel 30 at T=25°C (V_{OP}=57.46V, DAC=966ch).

As apparent, the baseline pedestal, first photoelectron and second photoelectron pulses for the LCT-1 SiPM are clearly visible, thus demonstrating superior detector performance, confirming the functionality of the SiPM boards, and validating the adopted measurement procedure.

6. CONCLUDING REMARKS

Test reliability measurements through pulse height distributions of the SiPM macro-pixels of the telescope focal plane have been performed to assess the functionality of the SiPM I/F boards design and the detector soldering technique.

Photoelectron resolution resulting from the performed measurements turned out to be poor, due to the low gain value of the MPPC detectors and the EASIROC fast shaper gain stage, and because of the grouping of four 3mm×3mm SiPM pixels, which drastically reduces the pulse amplitude of the signal waveform.

Indeed, dark stairs could not be performed with the MPPC detectors of the ASTRI SST-2M focal plane, because the EASIROC electronics is not capable of discriminating the single photoelectron pulses.

However, the reliability of the SiPM boards in terms of design and assembling has been confirmed. In fact, the same pulse height distribution measurements with the same EASIROC electronics have been carried out with an MPPC detector with a higher gain (in the order of 10^6), showing good photoelectron resolution.

7. CONTACTS

The team working on the electronic design of the ASTRI camera is composed by people from INAF's Catania Astrophysical Observatory and Palermo IFC. It is also referred to as the Electronics Camera Team.

Giovanni Bonanno	gbo@oact.inaf.it	OACT Catania
Giuseppe Romeo	giuseppe.romeo@oact.inaf.it	OACT Catania
Salvatore Garozzo	salvatore.garozzo@oact.inaf.it	OACT Catania
Davide Marano	davide.marano@oact.inaf.it	OACT Catania
Alessandro Grillo	agrillo@oact.inaf.it	OACT Catania
Sergio Billotta	sergio.billotta@oact.inaf.it	OACT Catania
Osvaldo Catalano	osvaldo.catalano@iasf-palermo.inaf.it	IFC Palermo
Giovanni La Rosa	larosa@ifc.inaf.it	IFC Palermo
Giuseppe Sottile	sottile@ifc.inaf.it	IFC Palermo
Salvatore Giarrusso	jerry@ifc.inaf.it	IFC Palermo
Domenico Impiombato	domenico.impiombato@ifc.inaf.it	IFC Palermo